Geophysical Research Letters

Supporting Information for

Mars Soil Temperature and Thermal Properties from InSight HP3 Data

T. Spohn[1], N. Müller[1], J. Knollenberg[1], M. Grott[1], M. P. Golombek[2], A.-C. Plesa[1], V. T. Bickel[3], P. Morgan[4], C. Krause[5], D. Breuer[1], S. E. Smrekar[2], W. B. Banerdt[2,*]

[1]Institute of Planetary Research, German Aerospace Center DLR, Rutherfordstrasse 2, 12489 Berlin, Germany.

[2]Jet Propulsion Laboratory, California Institute of Technology, 4800 Oak Grove Drive, Pasadena, 91109, California, USA.

[3]Center for Space and Habitability, University of Bern, Gesellschaftsstrasse 6, Bern, 3012, Switzerland.

[4]Colorado Geological Survey, Colorado School of Mines, 1801 19th St., Golden, 80401, Colorado, USA.

[5]MUSC Space Operations and Astronaut Training, German Aerospace Center DLR, Linder Höhe, Köln, 51147, Germany.

Contents of this file

*Present address: 1854 Clayton Ave., Pittsburg, 15214, Pennsylvania, USA

Introduction

This file contains two pieces of text S1 and S2 with embedded figures S1-S4 to supplement the information given in the main paper. Text S1 gives a detailed description of the HP^3 sensors on the thermal probe – the mole – and the radiometer used to measure the temperatures reported in the paper. S2 describes in detail how the surface and sub-surface temperatures were used to calculate the thermal diffusivity and the depth to the mole from the diurnal and annual thermal waves.

Text S1.

Thermal Sensors

For measuring soil temperature, we use the two TEM-A sensors on the HP^3 thermal probe – the mole (compare Fig. S1) - that were originally designed to measure the thermal conductivity (Spohn et al., 2018; Grott et al., 2019, 2021, 2023) with a modified line heat source method. The TEM-A sensors consist of thin copper wires densely printed on Kapton™ foil shells (compare Fig. S2). The shells are glued with Scotchweld™ 2216 onto the mole hull and protected against abrasion by a cover foil. The surface area of a TEM-A sensor is 12,000 mm^2, the copper wires have a width of 142.5 μm, and the spacing between tracks is 150 μm. The resistance of the wires is temperature dependent with a temperature coefficient of resistance of 0.00415 K^{-1}. The resistance is measured using the Kelvin 4-wire technique. The difference between the two TEM-A foil temperatures was <0.1 K.

The sensor can be heated by applying a predetermined power that is kept constant during a thermal conductivity measurement while the resistance is measured and converted to temperature. The rate of temperature increase after a transitory period can then be inverted to give the thermal conductivity (e.g., Grott et al., 2019, 2021). Prior to a thermal conductivity measurement and before the heater power was switched on, the soil temperature was recorded for two half and a full Martian sol. A solar day (sol) on Mars is 24 Mars hours of 61.65 minutes or 88775 seconds. The sols are counted starting with the landing of InSight on sol 0. We use the recordings of the full sol for the present paper.

In addition to the TEM-A data, we use temperature measurements of a housekeeping (H/K) sensor glued to the back of the mole motor (compare Fig. S1). The sensor together with a separate dedicated heater were designed to control the mole motor temperature and keep the motor in its specified operations range. The motor temperature was continuously recorded while the instrument was switched on in the first year on Mars. The dwindling resources in the second Martian year motivated a reduction in operation time to two times per sol for a total of 94 sols, at 6:00 LTST (Local True Solar Time) and at 13:00 LTST.

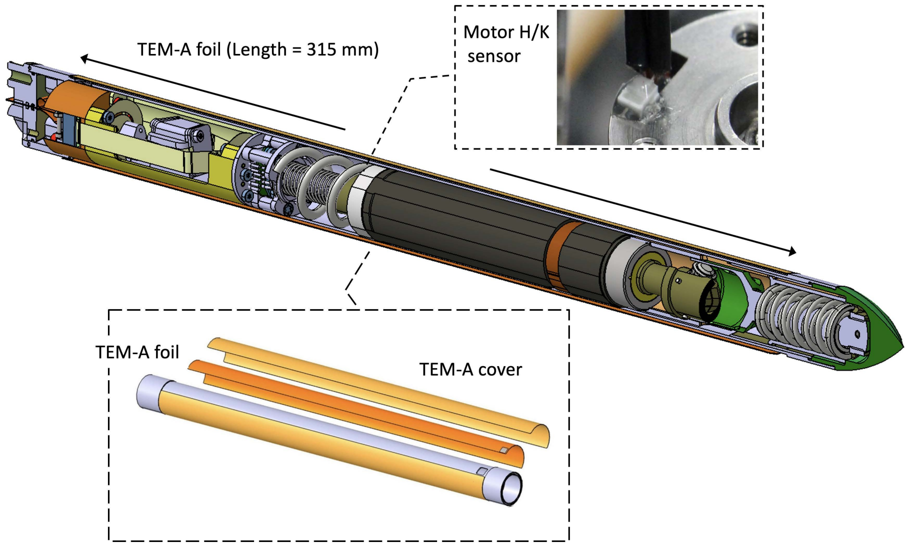

Figure S1. View of the internals of the HP^3 mole showing the extent of a TEM-A sensor foil (orange) and where it is located. The TEM-A foils are mounted 27 mm above the back end of the mole and extend for 315 mm. In addition, the location of the mole motor H/K temperature sensor is shown, 173 mm above the back end. The mole has a total length of 400 mm, a diameter of 27 mm, and a mass of 860 g.

The mole motor temperature sensor is a P1K0.232.6W.B.010 commercial, pre-wired RTD Platinum Sensor that meets the ECSS-Q-ST-60C Class 2 requirements. The operating temperature ranges from -200 °C to +600 °C. Its nominal resistance is 1000 Ohm at 0 °C and its dimensions are 2.3 mm x 2 mm x 1.3 mm (L x W x H). Its tolerance class is F0.3. The sensor is run in two-wire configuration (as compared with a four-wire configuration for the TEM-A sensors). Accordingly, the temperature dependence of the electrical wiring running to the sensor contributes to the error. The sensor was glued to the motor before integration to warrant a good thermal coupling. The motor H/K temperature sensor is located about halfway along the length of the two TEM-A foils but off-center, close to one of the two. This break in symmetry had no obvious effect on the temperature measurements.

The calibration of the TEM-A sensor in the range between 198.15 and 328.15 °C has been described in Grott et al (2019). The measurement uncertainty was found to be 30 mK at the 1σ level at the time of calibration. The sensors did drift by up to 0.25 K under thermal stress during 257 cycles between 183.15 and 298.15 °C and 26 cycles between 153.15 and 348.15 °C. While temperature drift uncertainty is a minor contribution to the total thermal conductivity uncertainty budget, it dominates the uncertainty budget for measuring the absolute soil temperature which is about 0.1 K.

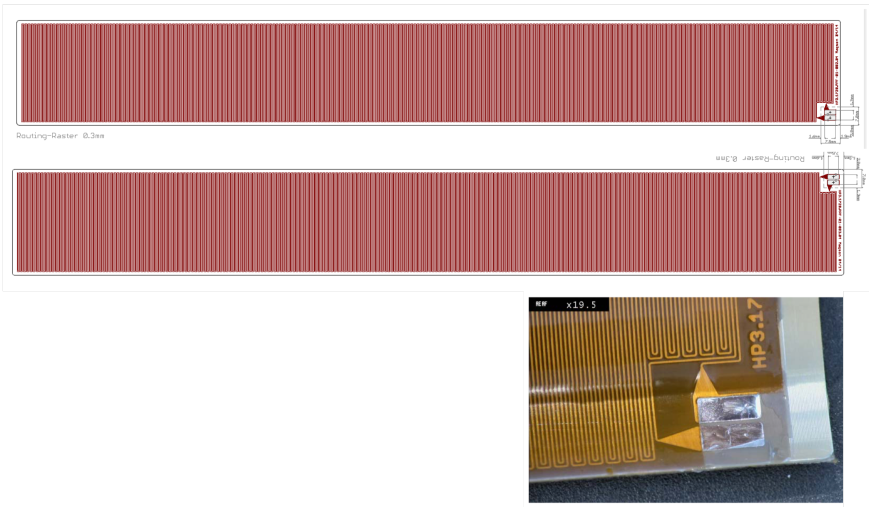

Figure S2. Layout of the wiring on a TEM-A sensor foil. The foils are 315 mm long and are mounted 27 mm below the back end of the mole. The copper wires have a width of 142.5 µm, and the spacing between tracks is 150 µm.

The H/K sensor was calibrated at the DLR Institute of Planetary Research during thermal vacuum tests of the HP^3 Proto-Flight-Model-2. The calibration was documented in HP^3Insight-DLR-TR-0907, "SSA PFM-2 Thermal Vacuum Test Report". The uncertainty of the H/K sensor readings was estimated to be 2 K (2σ level) under realistic operational conditions. The H/K sensors have been re-calibrated for this paper using the recordings of the TEM-A and the TEM-P sensors on the science tether (Spohn et al., 2018) and assuming that the harness running to the electronic box above the surface were of the same temperature as the TEM-P sensors.

The HP^3 radiometer RAD has been described in Spohn et al (2018) and its calibration in Müller et al. (2020). It is mounted underneath the lander deck facing south, opposite to where the HP^3 mole is located. HP^3 RAD has six thermopile sensors observing two spots on the surface. Field of view (FOV) 1 is closer to the lander and FOV 2 about 4m away from the center of the lander. Because the lander shadow and its thermal environment perturb the observation at FOV 1, FOV 2 is used here. Of the three sensors per FOV covering different bandwidths, we use the broadband 8-14 µm sensor. The latter is least affected by systematic calibration issues as reported in Müller et al (2020). The brightness temperature is converted to temperature using an emissivity of 0.98 ± 0.2 (Morgan et al., 2018). The uncertainty of the temperature varies through the sol with the environment temperature. Overall, it was estimated to be 3 K for the 24h average. With 3 K for the 6:00 LTST and 1.5 K for the 13:00 LTST measurements, the uncertainty of the average of these two is 2 K. This estimate also applies to the difference between the two as used for the diffusivity derived from the diurnal wave. Since a significant part of the uncertainty is non-random but systematic, temperature differences as needed for the calculation of the thermal diffusivity from the annual wave should be subject to an uncertainty of <1 K.

Text S2.

Thermal Diffusivity and Mole Depth from Diurnal and Annual Thermal Wave Data

In the following, we describe how the surface and soil temperature recordings were used to estimate the soil thermal diffusivity and the depth to the mole upper end (compare Spohn, 2024). Note that the depth to the mole was not well known before but was estimated to be 1-2 cm from camera data (Spohn, Hudson, Marteau et al., 2022).

It is well known [e.g., Carslaw and Jaeger, 1959) that the peak-to-peak temperature oscillation in a half-space heated periodically at the surface decreases with $exp(z/\delta)$, where z is depth and where $\delta = \sqrt{\kappa P/\pi}$ is the thermal skin depth, with P the period of the forcing temperature variation. Since the mole is an extended thermal sensor, it will average the temperature along its length. Averaged over the depth interval sampled by the mole, we get for the peak-to-peak variation $\overline{\Delta T}$

$$\overline{\Delta T} = \frac{1}{z_1 - z_0}\int_{z_0}^{z_1} \Delta T(z=0) \cdot exp\,(\frac{z_0}{\delta})\,dz \qquad \text{(S1)}$$

where z_0 is the depth to the mole back-end and z_1 the depth to the tip. Let $l' \equiv\ l\,cos\,i$, where l is the length of the mole (40 cm) and i its inclination with respect to vertical (30 ± 0.22° (Grott et al., 2019; Spohn, Hudson, Marteau et al., 2022) after the complete burial of the mole), then $z_1 = z_0 + l'$ and

$$\chi \equiv \frac{\overline{\Delta T}}{\Delta T(z=0)} = \frac{\delta}{l'}\left(1 - exp(-\frac{l'}{\delta})\right) \cdot exp\,(-\frac{z_0}{\delta}) \qquad \text{(S2)}$$

With $x \equiv l'/\delta$, $y \equiv z_0/\delta$, and $C \equiv x/(e^x - 1)$, we get from (S2)

$$\ln\chi + \ln C = -y - x \qquad \text{(S3)}$$

The phase lag Φ of the temperature variation increases with depth according to z/δ (e.g., Carslaw and Jaeger, 1959). Because the temperature signal decreases exponentially along the mole, we calculate the average value of the phase lag by taking a weighted average over the depth extent of the mole:

$$\overline{\Phi} = \frac{\frac{1}{\delta}\int_{z_0}^{z_1} z \cdot e^{-(z-z_0)/\delta} dz}{\int_{z_0}^{z_1} e^{-(z-z_0)/\delta} dz} \qquad \text{(S4)}$$

$$= y + 1 - C \qquad \text{(S5)}$$

For the diurnal wave, we note that the thermal skin depth δ_d is expected to be significantly smaller than l' and thus $x >> 1$. C will then be very close to zero and can safely be neglected in Equ. S5 for the diurnal wave. The phase lag measured by TEM-A will then be close to the phase lag at depth $z = z_0 + \delta_d$. Moreover, Eqn. S3 for the diurnal wave transforms to

$$\ln \chi + \ln x = -y \tag{S6}$$

The diurnal and annual thermal skin depths, respectively, are given by:

$$\delta_d = \sqrt{\frac{\kappa P_d}{\pi}} \tag{S7}$$

$$\delta_a = \sqrt{\frac{\kappa P_a}{\pi}} \tag{S8}$$

where P_d is a sol and P_a a Martian year in seconds.

The skin depths of the diurnal and annual waves differ by a factor of the square root of the number of sols in the Martian year (≈ 26, for a constant thermal diffusivity) and thus sample different depth ranges. Therefore, we use the amplitude ratios and the phase lags of the diurnal and annual waves separately to calculate values of κ representative of the different depth ranges. We use the diurnal wave to estimate z_0 which can be done with a reasonable uncertainty of about 4% as we will show below. The uncertainty of estimating z_0 from the annual wave was found to be unreasonably large, however, mostly because of the uncertainties of the data and the large difference between z_0 and δ_a.

For the diurnal wave, we use the six TEM-A 24h recordings available for sols 796 - 1202 as shown in Fig. 2 (top) of the main paper. As described in the main paper we use the following combinations of RAD/TEM-A data 120/796, 138/825, 174/872, 511/1202, 1075/1069, and 1175/1157. Fig. S3 shows the temperature centered around the daily average and scaled by the difference between the maximum temperature and the average temperature for the pairs of sols considered for the analysis. For the phase shifts, we use Fourier analyses (with Microsoft Excel™) of the recordings and the phase shifts (in Mars hours of 3699s) between the fundamental modes. The amplitude ratios for the full signals and the fundamental modes differ by a few percent only. Fig. 3 of the main paper shows the solutions to Eqn. 5 (with $C = 0$) and 6 in terms of z_0 and κ after de-trending for a temperature dependence of the measured amplitude ratio and the phase lag and a dependence of the phase lag on the amount of mismatch of the sols used for the analysis. We find the top-most piece of the mole to be at a depth of 5.07 ± 0.25 mm and the thermal diffusivity to be $2.30 \pm 0.03 \times 10^{-8}$ m^2 s^{-1}. Considering the diameter of the mole of 13.5 mm and its inclination towards vertical of 30 ± 0.22°, the center of the back-cap is at a depth of 11.8 ± 0.3 mm. The thermal skin depth is found to be 25 ± 0.4 mm and the wavelength 160 mm.

To estimate the uncertainties of the values of z_0 and κ we take the uncertainty of the temperature differences measured by the TEM-A sensor to be 0.1 K (Grott et al., 2019) and 2 K for the temperature differences measured by RAD. The InSight clocks measured time to better than 10^{-3} s and thus we take the discretization time step as indication of the uncertainty for the phase differences. We had more than 5000 time steps available for the TEM-A data but for RAD only the recordings at sols 120, 1075 and 1175 were of a similar time resolution. For sols 138, 174 and 511, about 550 time steps were recorded. Thus, we used 512 data points for the combinations of sols 138/825, 174/872 and 511/1202. For these, the relative uncertainties are 7% for z_0 and 6% for κ. For the combinations of sols 120/796, 1075/1069, and 1157/1175 we used 4096 data points resulting in relative uncertainties of 3% for z_0 and 5% for κ. The uncertainties are shown as error bars in Fig. 3 of the main paper along with the mean values calculated from the data points and their standard deviations of 5% for z_0 and 1.3% for κ, respectively. The above uncertainties are smaller than the scattering of the values around the mean. The standard deviation from the mean was found to be about 12% for z_0 and 3% for κ, similar to the average absolute spread about the mean value of 9.5% and 2.6%, respectively.

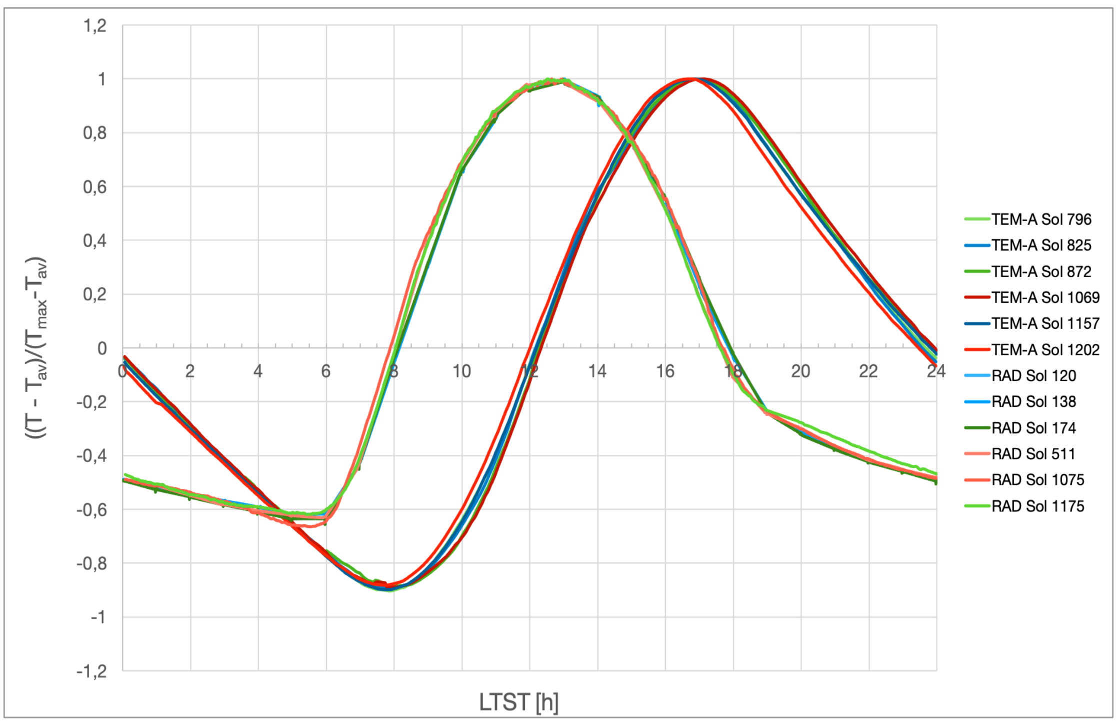

Figure S3. Scaled and centered mole temperature (indicated by the label "TEM-A" and the sol number) and surface temperature (indicated by the label "RAD" and the sol number) as functions of Local True Solar Time LTST in Mars hours. T_{av} is the 24h-averaged temperature and T_{max} the maximum temperature on the specified sol. The temperature scale $T_{max} - T_{av}$, is between 2.8 and 3.5 K for TEM-A and between 55.5 and 65.4 K for the surface temperature, respectively.

The data for the annual wave are significantly noisier than the diurnal wave recordings, which should partly be a consequence of the weather on Mars. A total of 1.81 Martian years (1231 sols) of surface temperatures are available but only 565 sols (0.85a) of buried mole data and only 459 sols (0.69a) after the Free Mole Test with the final hammering (compare Fig. 2 of the main paper).

The data used to estimate the phase shift between the surface and mole signal from a Fourier analysis of the signal are shown in Fig. S4. Because only about 2/3 of a Martian year of data are available, the data vector was filled with zeros symmetrically at the beginning and the end of the vector, as is commonly done for numerical Fast Fourier Transforms. The time resolution of the data set is 669:512 sols. The analysis resulted in an estimate of the phase lag of 20.9 sols with an estimated uncertainty of ±2 sols.

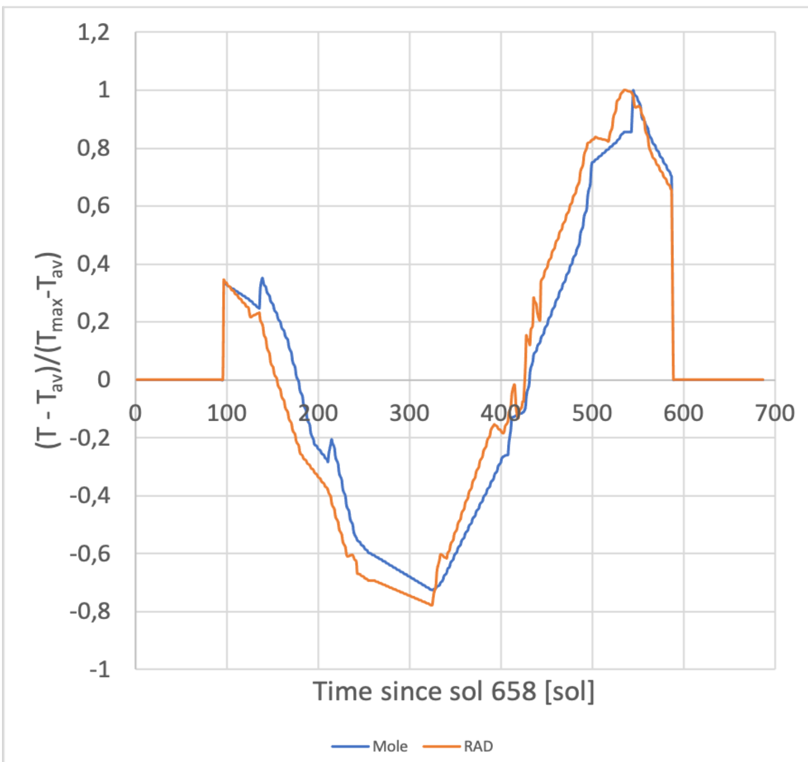

Figure S4. Scaled and centered surface (red) and mole (blue) temperature in the time window between sols 754 and 1245 for which data are available. The time intervals between sols 658 and 754 and 1245 and 1316 have been filled with zero values to perform a numerical Fast Fourier Transform. The temperature scale $T_{max} - T_{av}$, where T_{max} is the annual maximum temperature and T_{av} the yearly average is 7.65 K for the mole and 9.14 K for the surface temperature. The phase lag was determined by Fourier analysis to be 20.9 sols.

With the above uncertainty of the phase lag and an uncertainty of 1K for the annual temperature variations at the surface and at mole depth, we find from the amplitude ratio a thermal diffusivity of $3.68 \pm 1.1 \times 10^{-8}$ m^2 s^{-1} and of $3.80 \pm 0.51 \times 10^{-8}$ m^2 s^{-1} 3.80 from the phase lag. Taking the average value of the two, we calculate a thermal skin depth of 84 ± 10cm and a wavelength of 5.3m.